

On the Limits of Digital Back-Propagation in the Presence of Transceiver Noise

LIDIA GALDINO,^{1,*†} DANIEL SEMRAU,^{1,†} DOMANIÇ LAVERY,¹
GABRIEL SAAVEDRA,¹ CRISTIAN B. CZEGLEDI,² ERIK AGRELL,²
ROBERT I. KILLEY,¹ AND POLINA BAYVEL¹

¹*Optical Networks Group, Department of Electronic and Electrical Engineering, UCL, Torrington Place, London WC1E 7JE, UK*

²*Department of Signals and Systems, Chalmers University of Technology, Gothenburg, SE-412 96, Sweden*

*l.galdino@ucl.ac.uk

Abstract:

This paper investigates the impact of transceiver noise on the performance of digital back-propagation (DBP). A generalized expression to estimate the signal-to-noise ratio (SNR) obtained using DBP in the presence of transceiver noise is described. This new expression correctly accounts for the nonlinear beating between the transceiver noise and the signal in the optical fiber transmission link. The transceiver noise-signal nonlinear beating has been identified as the main reason for the discrepancy between predicted and practical performance of DBP; which has not been previously suggested. This nonlinear beating has been included in the GN model, allowing DBP gains in practical systems to be predicted analytically. Experiments and split-step simulations with and without polarization-mode dispersion (PMD) in the transmission link have been performed. The results show that the impact of transceiver noise greatly outweighs that of PMD, and the analytical expressions are confirmed by the numerical simulations.

© 2016 Optical Society of America

OCIS codes: (060.1660) Coherent communications; (060.2330) Fiber optics communications.

References and links

1. R. Maher, A. Alvarado, D. Lavery, and P. Bayvel, "Increasing the information rates of optical communications via coded modulation: a study of transceiver performance," *Sci. Rep.* **6**, 21278 (2016).
2. Xi Chen, S. Chandrasekhar, S. Randel, W. Gu, and P. Winzer "Experimental Quantification of Implementation Penalties from Limited ADC Resolution for Nyquist Shaped Higher-Order QAM," in Proc. of Optical Fiber Communication Conference (OFC), W4.A.3 (2016).
3. E. Ip, "Nonlinear compensation using backpropagation for polarization-multiplexed transmission," *J. Lightw. Technol.* **28**(6), 939–951 (2010).
4. A. D. Ellis, M. E. McCarthy, M. A. Z. Al-Khateeb, and S. Sygletos, "Capacity limits of systems employing multiple optical phase conjugates," *Opt. Express* **20**(16), 20381–20393 (2015).
5. G. Gao, X. Chen, and W. Shieh, "Influence of PMD on fiber nonlinearity compensation using digital back propagation," *Opt. Express* **20**(13), 14406–14418 (2012).
6. G. Liga, C. B. Czegledi, T. Xu, E. Agrell, R. I. Killey, and P. Bayvel, "Ultra-wideband nonlinearity compensation performance in the presence of PMD," in Proc. of European Conference on Optical Communication (ECOC), 794–796 (2016).
7. R.-J. Essiambre and P. J. Winzer, "Fibre nonlinearities in electronically pre-distorted transmission," in Proc. of European Conference on Optical Communication (ECOC), Tu.3.2.2 (2005).
8. Z. Tao, L. Dou, W. Yan, L. Li, T. Hoshida, and J. C. Rasmussen, "Multiplier-free intrachannel nonlinearity compensating algorithm operating at symbol rate," *J. Lightw. Technol.* **29**(17), 2570–2576 (2011).
9. A. Ghazisaeidi and R.-J. Essiambre, "Calculation of coefficients of perturbative nonlinear pre-compensation for Nyquist pulses," in Proc. of European Conference on Optical Communication (ECOC), We.1.3.3 (2014).
10. M. Secondini, D. Marsella, and E. Forestieri, "Enhanced split-step fourier method for digital backpropagation," in Proc. of European Conference on Optical Communication (ECOC), We.3.3.5 (2014).
11. X. Liang and S. Kumar, "Multi-stage perturbation theory for compensating intra-channel nonlinear impairments in fiber-optic links," *Opt. Express* **22**(24), 29733–29745 (2014).
12. R. Dar and P. J. Winzer, "On the limits of digital back-propagation in fully loaded WDM systems," *Photon. Technol. Lett.*, **28**(11), 1253–1256 (2016).
13. T. Tanimura, M. Nölle, J. K. Fischer, and C. Schubert, "Analytical results on back propagation nonlinear compensation with coherent detection," *Opt. Express* **20**(27), 28779–28785 (2012).

14. X. Liang and S. Kumar, "Multi-stage perturbation theory for compensating intra-channel nonlinear impairments in fiber-optic links," *Opt. Express* **22**(24), 29733–29745 (2014).
15. R. Maher, T. Xu, L. Galdino, M. Sato, A. Alvarado, K. Shi, S. J. Savory, B. C. Thomsen, R. I. Killey, and P. Bayvel, "Spectrally shaped DP-16QAM super-channel transmission with multi-channel digital back-propagation," *Scientific Reports* **5**, 8214 (2015).
16. E. Temprana, E. Myslivets, L. Liu, V. Ataie, A. Wiberg, B. P. P. Kuo, N. Alic, and S. Radic, "Two-fold transmission reach enhancement enabled by transmitter-side digital backpropagation and optical frequency comb-derived information carriers," *Opt. Express* **23**(16), 20774–2783 (2015).
17. C. Lin, S. Chandrasekhar and P. J. Winzer, "Experimental study of the limits of digital nonlinearity compensation in DWDM systems," in Proc. of Optical Fiber Communication Conference (OFC), Th4D.4, (2016).
18. E. Temprana, E. Myslivets, V. Ataie, B. P. -P. Kuo, N. Alic, V. Vusirikala, V. Dangui and S. Radic, "Demonstration of coherent transmission reach tripling by frequency-referenced nonlinearity pre-compensation in EDFA-only SMF link," in Proc. of European Conference on Optical Communication (ECOC), p376, (2016).
19. D. Lavery, D. Ives, G. Liga, A. Alvarado, S. J. Savory, and P. Bayvel, "The benefit of split nonlinearity compensation for single channel optical fiber communications," *Photon. Technol. Lett.* **28**(17), 1803–1806 (2016).
20. A. Ghazisadeidi, I. Ruiz, L. Schmalen, P. Tran, C. Simonneau, E. Awwad, B. Uscumlic, P. Brindel, and G. Charlet, "Submarine transmission systems using digital nonlinear compensation and adaptive rate forward error correction," *J. Lightw. Technol.* **34**(8), 1886–1895 (2016).
21. P. Poggiolini, G. Bosco, A. Carena, V. Curri, Y. Jiang, and F. Forghieri, "The GN-model of fiber non-linear propagation and its applications," *J. Lightw. Technol.* **32**(4), 694–721 (2014).
22. P. Poggiolini, G. Bosco, A. Carena, V. Curri, Y. Jiang, and F. Forghieri, "A simple and effective closed-form GN model correction formula accounting for signal non-Gaussian distribution," *J. Lightw. Technol.* **33**(2), 459–473 (2015).
23. A. D. Ellis, S. T. Le, M. A. Z. Al-Khateeb, S. K. Turitsyn, G. Liga, D. Lavery, T. Xu, and P. Bayvel, "The impact of phase conjugation on the nonlinear-Shannon limit: the difference between optical and electrical phase conjugation," in Proc. of IEEE Summer Topicals Meeting Series, 209–210 (2015).
24. X. Liu, A. R. Chraplyvy, P. J. Winzer, R. W. Tkach, and S. Chandrasekhar, "Phased-conjugated twin waves for communication beyond the Kerr nonlinearity limit," *Nature Photonic*, **7**(7), 560–568 (2013).
25. T. Xu, G. Liga, D. Lavery, B. C. Thomsen, S. J. Savory, R. I. Killey and P. Bayvel, "Equalization enhanced phase noise in Nyquist-spaced superchannel transmission systems using multichannel digital back-propagation," *Scientific Reports*, **5**, 13990 (2015).
26. D. Marcuse, C. R. Menyuk, and P. K. A. Wai, "Application of the Manakov-PMD equation to studies of signal propagation in optical fibers with randomly varying birefringence," *J. Lightw. Technol.* **15**(9), 1735–1746 (1997).
27. S. Chandrasekhar, B. Li, J. Cho, X. Chen, E. C. Burrows, G. Raybon, and P. J. Winzer, "High-spectral-efficiency transmission on PDM 256-QAM with parallel probabilistic shaping at record rate-reach trade-offs," in Proc. of European Conference on Optical Communication (ECOC), postdeadline paper Th.3.C.1, (2016).

1. Introduction

An upper bound on the achievable signal-to-noise ratio (SNR) in coherent optical communication systems is set by the noise introduced by the transceiver subsystems [1, 2]. Significant sources of transceiver noise include quantization noise due to the finite resolution of digital-to-analog converters (DAC) and analog-to-digital converters (ADC), and the noise contribution from the linear electrical amplifiers.

The achievable SNR is further limited by the nonlinear signal distortion, inherent to transmission through an optical fiber communication system. Several nonlinear compensation (NLC) schemes have been proposed to mitigate this effect, of which the digital back-propagation (DBP) algorithm is a promising candidate [3]. DBP is known to compensate deterministic nonlinear signal self-interactions (e.g., self-phase modulation); however, this algorithm is unable to compensate for any signal-noise interactions, which occur due to the amplified spontaneous emission (ASE) noise added by optical amplifiers along the transmission link [4]. Similarly, other stochastic effects, such as polarization mode dispersion (PMD), impose a limitation on the performance of DBP [5, 6].

Several NLC algorithms based on DBP have been proposed in the literature [3–14], showing that significant SNR gains can be potentially achieved when full-field DBP (FF-DBP) is applied (DBP is applied jointly to all received channels). However, numerical simulations [5, 6] show a marked decrease in the performance of DBP when the signal is propagated in the presence of PMD. Despite the DBP gain degradation caused by PMD, theoretical predictions still sub-

stantially overestimate the experimentally achieved system performance (cf. [5, 6] and [15–18]), suggesting that additional channel impairments must be considered when estimating the DBP performance.

In this paper, we seek to account for this discrepancy by investigating the limits of DBP in realistic optical transmission systems, in which a limit on the maximum achievable SNR is imposed through the introduction of system impairments (herein referred to as transceiver noise). A new expression to estimate the SNR after DBP in the presence of transceiver noise is presented, and an inequality is derived that estimates the regime in which the transceiver noise-signal interactions are dominant compared to the ASE noise-signal interactions. The modified analytical model is compared to split-step simulations and experimental data. Furthermore, the gain degradation due to transceiver noise is compared to that arising from PMD. The theoretical results are further extended to C-band transmission. The implications of the ratio of the transceiver noise between the transmitter and the receiver on the impact of transmitter-side DBP (predistortion), receiver-side DBP and split DBP (an equal division of DBP between transmitter and receiver) [19] are also investigated.

This paper is organized as follows. In Section 2, the analytical model is described and an inequality is derived that estimates the transceiver SNR below which transceiver noise-signal interactions must be considered. Section 3 presents the experimental configuration and split-step simulation methodology. The transmission performance for the experimental data, split-step simulations with and without PMD in the transmission link and the proposed analytical model are analysed in Section 4. The DBP performance for a C-band transmission system in the presence of transceiver-limited SNR is presented in Section 5, with key conclusions summarised in Section 6.

2. Analytical Model

In this section a generalized formula for the SNR that accounts for the transceiver noise and, in particular, the interactions between the signal and the co-propagating transceiver noise, is presented. Additionally, a simple inequality is derived that estimates the required transceiver SNR beyond which the transceiver noise-signal beating can be neglected.

When only a linear electronic dispersion compensation (EDC) filter is applied to the signal, the SNR_{EDC} after transmission is dominated by three separate, independent, noise components: nonlinear interference noise variance σ_{NLI}^2 , ASE noise variance σ_{ASE}^2 and transceiver noise variance σ_{TR}^2 . The noise after transmission can then be estimated as

$$\sigma_{\text{EDC}}^2 = \sigma_{\text{NLI}}^2 + \sigma_{\text{ASE}}^2 + \sigma_{\text{TR}}^2, \quad (1)$$

where the transceiver noise variance comprises the noise variance introduced by both the transmitter σ_{T}^2 and the receiver σ_{R}^2 as

$$\sigma_{\text{TR}}^2 = \sigma_{\text{T}}^2 + \sigma_{\text{R}}^2. \quad (2)$$

The noise terms from (1) can be included in the estimation of SNR for chromatic dispersion compensation only (SNR_{EDC}) in terms of the signal power P and its noise contributions as shown in [20, Eq. 11], and can be expressed as

$$\text{SNR}_{\text{EDC}} = \frac{P}{N^{1+\epsilon} \eta P^3 + \kappa P + N P_{\text{ASE}}}, \quad (3)$$

with the number of spans N , the coherence factor ϵ , the nonlinear interference (NLI) coefficient for one span η , the ASE noise power from each amplifier P_{ASE} and $\kappa P = \sigma_{\text{TR}}^2$. By definition, the transceiver SNR_{TR} is the maximum SNR that can be achieved in the transmission system in the

absence of NLI and ASE noise. We note that $\text{SNR}_{\text{TR}} = 1/\kappa$. This variable phenomenologically includes all impairments of the system under test and it can be measured in a back-to-back configuration without ASE noise loading. A detailed explanation of experimental impairments is given in subsection 4.1 in relation to this work.

In this work, the coherence factor is taken as a closed-form expression from the Gaussian-noise (GN) model [21, Eq. 40] and the NLI coefficient is taken from [21, Eq. 36] where we partly corrected for the modulation format dependence with the formula given in [22, Eq. 2]. The maximum SNR_{EDC} for EDC only can be obtained from (3) via straightforward algebra as

$$\max_P(\text{SNR}_{\text{EDC}}) = \frac{1}{\kappa + \sqrt[3]{\frac{27}{4} P_{\text{ASE}}^2 \eta N^{3+\epsilon}}}. \quad (4)$$

In the case of EDC only, the launch power that maximizes the SNR is independent of the transceiver noise.

In order to account for DBP (or NLC in general), (3) must be modified. In particular, DBP decreases the NLI coefficient and therefore ASE noise-signal interactions, which were neglected previously, must be taken into consideration. The resulting SNR for DBP, assuming ideal, noiseless transceivers, can be estimated as [23, Eq. 2] and [13, Eq. 1-6]. In order to account for transceiver impairments (hereafter termed transceiver noise) a linear contribution has to be added, similar to the EDC case in (3), as well as a nonlinear beating term that accounts for the beating between the signal and transceiver noise. To the best of the author's knowledge this beating term has not been considered in previous literature. Accounting for both noise contributions a generalized expression for the SNR estimation can be written as

$$\text{SNR} = \frac{P}{(N^{1+\epsilon} \eta - N^{1+\epsilon_{\text{NLC}}} \eta_{\text{NLC}}) P^3 + \kappa P + NP_{\text{ASE}} + 3\eta(\xi_1 P_{\text{ASE}} + \xi_2 \kappa_R P) P^2}, \quad (5)$$

where η_{NLC} and ϵ_{NLC} are the NLI coefficient and the coherence factor for the back-propagated signal, respectively. The quantities ξ_1 , ξ_2 and κ_R depend on the ratio between transmitter and receiver noise, and also on where the DBP is applied; transmitter-side, receiver-side or split-DBP. Assuming lumped amplification and receiver-side DBP, the first and second coefficient of the beating term are given by $\xi_1 = \sum_{k=1}^N k^{1+\epsilon}$ and $\xi_2 = N^{1+\epsilon}$ [19], respectively. Furthermore, assuming that the transceiver noise is split equally between transmitter and receiver, the quantity κ_R is given by $\kappa_R = \frac{1}{2}\kappa$. This analysis is generalized to any arrangement of nonlinearity compensation in the following subsection.

2.1. Origin of the virtual transceiver noise beating phenomenon

Fig.1 illustrates the accumulation of nonlinear signal-noise interactions along the transmission link. As described in (5), the transmitter noise σ_T^2 and receiver noise σ_R^2 introduce an additional nonlinear noise-signal beating. If DBP is applied at the receiver side, as shown in Fig. 1(a), it compensates only for the nonlinear beating noise introduced by the transmitter (red line). This noise beats with the signal along the entire physical forward link and the beating is reversed in the virtual backward link during DBP. The transmitter noise-signal beating is completely canceled as the physical and virtual link exhibit the exact same distance. However, the noise that is introduced by the receiver (blue line) only beats with the signal along the virtual link. Therefore, only the receiver noise contributes to the beating term in (5), for receiver-side DBP.

Although the preceding analysis is for receiver-side DBP only, it logically follows that if the nonlinearity compensation scheme were to be applied at the transmitter side, as illustrated in Fig.1(b), then it is the noise of the transmitter (orange line) that would give rise to transceiver noise-signal nonlinear beating. For transmitter-side DBP the first coefficient of the beating term is given by $\xi_1 = \sum_{k=1}^{N-1} k^{1+\epsilon}$ and ξ_2 is as defined above. Note that κ_R in (5) must be substituted

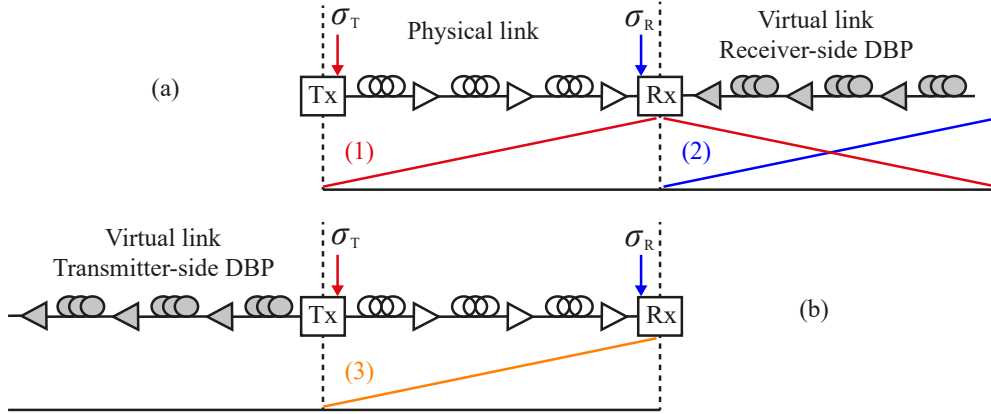


Fig. 1. Nonlinear signal-noise interactions accumulation along transmission link for (a) receiver-side DBP and (b) transmitter-side DBP. The colored lines show (1) nonlinear transmitter noise-signal beating, cancelled after DBP, (2) nonlinear receiver noise-signal beating, generated after DBP as: $3\eta\xi_2\kappa_R P^3$, and (3) nonlinear transmitter noise-signal beating, generated in transmission as: $3\eta\xi_2\kappa_T P^3$.

with the transmitter noise, κ_T , which again can be assumed to be half the transceiver noise, κ . Moreover, if the nonlinearity compensation is divided between transmitter and receiver (split-DBP), the transceiver noise-signal beating becomes a function of the noise at both the transmitter and the receiver. It should be noted that while the amount of ASE noise-signal beating can be minimized by split-DBP, the transceiver noise-signal beating is only weakly dependent on the split ratio.

If NLC is applied in the middle of the link (e.g., in the case of optical phase conjugation [23,24]) the beating between transmitter noise and signal in the first half of the link is inverted in the second half (and a virtual link is absent). It is, therefore, tempting to assume that NLC schemes that are located in the middle of the link would not suffer any SNR degradation from interactions between the signal and the transceiver noise. However, in practice, noiseless mid-link NLC may not be realizable and the uncompensated noise-signal interactions remain.

2.2. Implications on Full-Field Digital Back-Propagation (FF-DBP)

In this subsection, FF-DBP in the presence of transceiver SNR is studied and an inequality is derived that gives the required transceiver SNR below which transceiver noise-signal interactions must be taken into account. Moreover, in this regime the optimum launch power is different from the idealized case (without transceiver noise) and therefore, adding the transceiver noise *a posteriori* to an ideal analysis via (1) yields incorrect results. For FF-DBP $\eta = \eta_{NLC}$ and $\epsilon = \epsilon_{NLC}$ hold, and the proposed generalized SNR (5) reduces to

$$\text{SNR}_{\text{FF-DBP}} = \frac{P}{\kappa P + NP_{\text{ASE}} + 3\eta(\xi_1 P_{\text{ASE}} + \xi_2 \kappa_R P)P^2}. \quad (6)$$

The optimum launch power is obtained by setting the derivative of (6) to zero and solving the arising cubic equation. The optimum launch power is then substituted in (6) in order to obtain

the maximum $\text{SNR}_{\text{FF-DBP}}$. They are found to be

$$P_{\text{opt}} = \frac{\xi_1 P_{\text{ASE}} \phi}{6\xi_2 \kappa_R}, \quad (7)$$

$$\max_P(\text{SNR}_{\text{FF-DBP}}) = \frac{\xi_1 \phi}{(\phi + 6)\phi^2 \frac{\xi_1^3 P_{\text{ASE}}^2 \eta}{12\kappa_R N^{1+\epsilon}} + 6\kappa_R N^{2+\epsilon} + \xi_1 \kappa \phi}, \quad (8)$$

with

$$\phi = 2 \cosh \left[\frac{1}{3} \text{acosh}(\Gamma) \right] - 1, \quad (9)$$

$$\Gamma = \frac{18N^{3+2\epsilon} \kappa_R^2}{\xi_1^3 P_{\text{ASE}}^2 \eta} - 1. \quad (10)$$

The solution for the optimum launch power and the maximum $\text{SNR}_{\text{FF-DBP}}$ are exact and should be used when high accuracy is required. However, typical values in the field of optical communications yield $\Gamma \gg 1$ and ϕ can be approximated by $\phi \approx (2\Gamma)^{\frac{1}{3}} - 1$ (see Appendix).

We are now interested in the relationship between the amount of ASE noise-signal interactions $\xi_1 P_{\text{ASE}}$ and the transceiver noise-signal interactions $\xi_2 \kappa_R P$ in (6). The reason is that gains that are achieved by split-DBP or transmitter-side DBP (relative to receiver-side DBP) tend to zero in the regime of negligible ASE noise-signal interactions, as split DBP aims to minimize ξ_1 .

For $\Gamma \gg 1$, $N \gg 1$ and ϵ tends to zero [21], the relative amount of the two beating contributions can be expressed in terms of $\text{SNR}_{\text{EDC,ideal}}$, in the case that EDC only is applied and in the absence of transceiver noise. $\text{SNR}_{\text{EDC,ideal}}$ can be obtained from (4) by setting $\kappa = 0$. Assuming the mentioned relations and an equal split of transceiver noise between transmitter and receiver, and receiver-side DBP, the receiver noise-signal interactions can be neglected when

$$\max_P(\text{SNR}_{\text{EDC,ideal}})[\text{dB}] \ll \frac{2}{3} \text{SNR}_{\text{TR}}[\text{dB}] - 4.5 \text{dB}, \quad (11)$$

and the ASE noise-signal interactions can be neglected when

$$\max_P(\text{SNR}_{\text{EDC,ideal}})[\text{dB}] \gg \frac{2}{3} \text{SNR}_{\text{TR}}[\text{dB}] - 4.5 \text{dB}. \quad (12)$$

A more detailed derivation can be found in the Appendix. When inequality (11) is satisfied, an ideal analysis (simulative or analytical) can be carried out and transceiver noise can be added *a posteriori* via (1) because the transceiver noise contribution is independent from other noise terms. When inequality (12) is satisfied, gains due to split-DBP tend to zero as the only term that depends on ξ_1 becomes negligible.

3. Spectrally Shaped PDM-64QAM Superchannel Transmission System

Transmission experiments were performed to assess the impact of the transceiver noise-signal nonlinear beating on the performance of DBP, and to test the theory presented in the previous section.

The experimental configuration for the four-subcarrier 30 GBd polarization division multiplexing DP-64QAM transmission system is illustrated in Fig. 2. Four external cavity lasers (ECLs) with 100 kHz linewidth and 32 GHz frequency spacing were used as sources for two odd and two even subcarriers. The odd and even subcarriers were modulated using two separate IQ modulators, driven using spectrally shaped 64-QAM signals, with root raised cosine (RRC) filters with 0.1% roll-off from 92 GS/s DACs. Digital preemphasis was applied to the signal to compensate

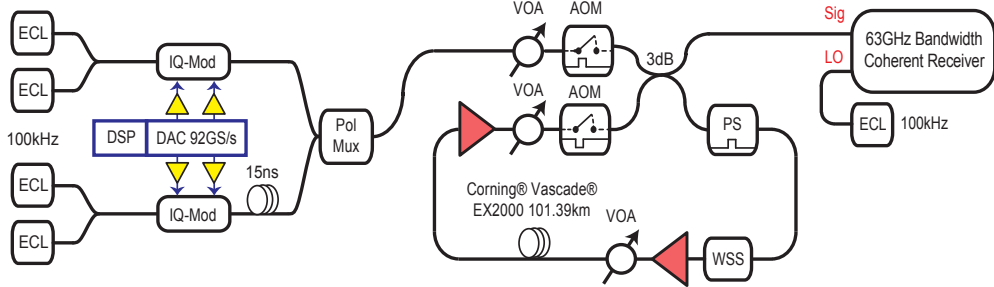


Fig. 2. Experimental configuration.

for the frequency response of the transmitter components. The odd and even subcarriers were decorrelated with a 15 ns delay before being combined in a polarisation-multiplexer (Pol. Mux.) to form a 4×30 GBd DP-64QAM superchannel.

For the back-to-back (BTB) analysis, the signal was passed directly to the coherent receiver. For transmission, a recirculating fiber loop was used, comprising a loop-synchronous polarization scrambler (PS), a single span of 101.39 km Corning® Vascade® EX2000 fiber with a total loss of 16.2 dB, an EDFA with 5 dB noise figure, a wavelength selective switch (WSS) for adjustable gain flattening, and a second EDFA to overcome the loop loss components (13.5 dB combined attenuation). A single high-bandwidth digital coherent receiver was used to detect all four subcarriers (allowing full-field receiver-side DBP). The received signal and local oscillator laser (LO), with 100 kHz linewidth, were combined using a 90° optical hybrid, followed by balanced photo-detectors with 70 GHz electrical bandwidth. The received signals were then digitized using two 160 GSa/s real-time digital sampling oscilloscopes with 63 GHz electrical analog bandwidth. The offline digital signal processing (DSP) implementation was as described in detail in [15]. This included receiver imbalance correction (which corrected the skew that was measured in advance using a frequency swept sine generated from the intradyne frequency offset between two lasers), digital backpropagation, adaptive equalization, and carrier recovery. The received total SNR was evaluated as the ratio between the variance of the transmitted symbols $E[|X|^2]$ and the variance of the noise σ^2 , where $\sigma^2 = E[|X - Y|^2]$ and Y represents the received symbols after DSP is applied.

The transmission setup described above was numerically simulated. The signal propagation over the optical fiber was simulated using the split-step Fourier method to solve the Manakov equation [26]. Two different simulation scenarios were analyzed: firstly, simulations assuming an idealized transceiver, without transceiver SNR limitation, and, secondly, transmission with transceiver limited SNR, assuming a practical SNR limit, which was measured in the BTB configuration, without ASE noise loading. The transceiver noise was assumed to be equally split between the transmitter and receiver. Additionally, in order to investigate the effectiveness of DBP in the presence of PMD in systems with a transceiver SNR limit, fiber propagation with and without the effect of PMD were both considered. The PMD parameter was chosen to be $0.05 \text{ ps}/\sqrt{\text{km}}$ according to fiber datasheet. A linear PMD equalizer operating with exact knowledge of the instantaneous PMD was used after the receiver-side DBP.

4. Superchannel transmission system

4.1. Back-to-back characterization

Fig. 3(a) illustrates the BTB experimentally measured received SNR as a function of OSNR, over both polarizations, for single channel only and for each subcarrier from the DP-64QAM

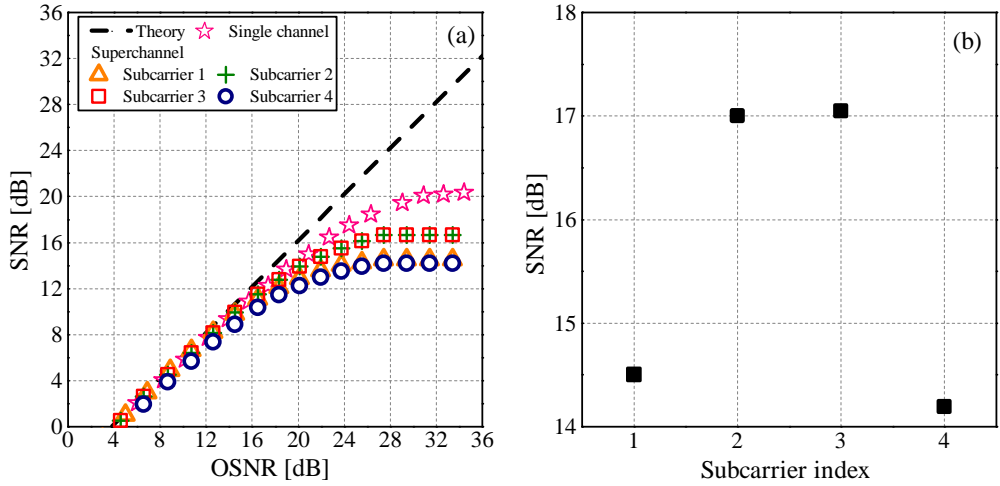


Fig. 3. BTB measurements (a) SNR vs. OSNR for single channel and each subcarrier of the superchannel; (b) maximum archivable SNR for each subcarrier.

superchannel. The subcarriers of the superchannel were simultaneously received, with the LO laser tuned to the superchannel centre frequency (between subcarriers 2 and 3), and individually down-converted to baseband in the digital domain before passing through to the remaining DSP functions. The theoretical calculation of $\text{OSNR} = \text{SNR} + 10 \log_{10}(R_s/B)$, where R_s is the symbol rate and B is the noise bandwidth, is also shown to provide a performance reference relative to the experimental results. It is evident in Fig. 3(a) that there is a saturation to the highest achievable SNR. The SNR for the single channel DP-64QAM format was limited to 20.5 dB because of a saturation in the SNR within the coherent optical transceiver. The main contributions to the limited SNR within the digital coherent transceiver were the DAC and the linear electrical amplifiers in the transmitter, and the ADC in the real time sampling oscilloscope at the receiver. The DAC exhibited a measured effective number of bits (ENOB) of 5 bits over a 15 GHz carrier frequency (the bandwidth of the spectrally shaped IQ drive signals), which corresponds to an SNR of approximately 32 dB. The linear amplifiers had a noise figure of 6 dB at a frequency of 15 GHz, therefore the maximum achievable SNR from the electrical components within the transmitter was approximately 26 dB. A further degradation of 2 dB for applying pulse shaping was observed, as it increases the peak-to-average power ratio of the QAM signal, exacerbating the transmitter impairments. The ADCs in the real time sampling oscilloscope also exhibited a frequency dependent ENOB, which was 4.8 bits at a frequency of 15 GHz (reducing to 4.3 bits at a frequency of 60 GHz). The additional loss in SNR was due to the inclusion of the optical components, strong signal pre-emphasis to overcome the limited IQ modulator bandwidth, and a blind DSP implementation. Additionally, as can be observed in Fig. 3(a), there is a further degradation in performance of 3.5 dB from single-channel to when every subcarrier of the superchannel is jointly received. As shown in Fig. 3(a) and (b) the further degradation in SNR for the highest and lowest frequency subcarriers was due to the inherent ENOB limitation of the ADCs at the receiver. We would like to point out that if the LO is centred on each subcarrier and each subcarrier is received individually, then each subcarrier has the same performance.

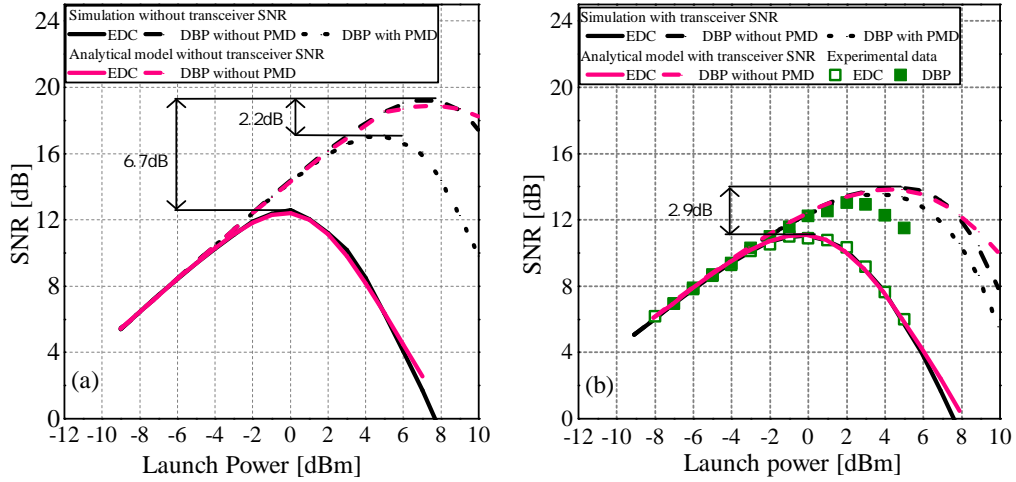


Fig. 4. Received SNR vs. subcarrier launch power over 5,000 km transmission (a) without transceiver noise and (b) with transceiver noise.

4.2. Superchannel transmission results

To confirm the theoretical predictions of the transceiver noise on the FF-DBP performance (see Section 2), split-step simulation and experiments of optical fiber transmission up to 5,000 km were carried out. All results shown in this subsection considered receiver-side FF-DBP. The loop configuration was also included in all sets of simulations and modelling in order to allow for direct comparison with the experimental data.

First, the performance of DBP without the presence of transceiver noise was analysed through simulations and compared to the analytical model. Fig. 4(a) shows the received SNR as a function of launch power for subcarrier 3 over 5,000 km for EDC only (solid line) and DBP with (dashed line) and without (dotted line) PMD along the transmission link. The black lines represent split-step simulations and the pink lines show the SNR predicted by the analytical model. The highest achievable SNR for EDC only is 12.4 dB at 0 dBm subcarrier launch power. When DBP in the absence of PMD was considered, the maximum SNR increases to 18.9 dB at 8 dBm subcarrier launch power, yielding a DBP gain of 6.7 dB. When PMD is included, an SNR decrease of 2.2 dB was observed. To study the performance of DBP in the presence of transceiver SNR limitation, simulations and modelling were carried out considering a maximum transceiver SNR of 17 dB, which was experimentally measured for subcarrier 3, allowing a direct comparison with experimental data. Simulations and modelling assumed that the transceiver noise is equally split between transmitter and receiver. The results for transmission over 5,000 km are shown in Fig. 4(b). The analytical model and simulation without PMD yield 2.9 dB gain in SNR when DBP is applied. This is a substantial decrease compared to the 6.7 dB gain in the case without transceiver noise. When PMD is included an additional penalty in SNR gain of 0.5 dB was observed; a strong contrast to the 2.2 dB penalty seen in simulations without transceiver limited SNR. This indicates that, for this sub-system, to up to 5,000 km the performance degradation due to transceiver noise is more significant than the degradation due to PMD. The experimental results are shown with open and solid markers for EDC only and DBP, respectively. Experimentally, a DBP gain in SNR of 2.0 dB was found compared to the 2.4 dB gain that was predicted by simulation (including PMD).

This slightly smaller gain and sharper performance degradation at higher launch powers may be due to the small mismatch of the dispersion values used in the DBP algorithm [16],

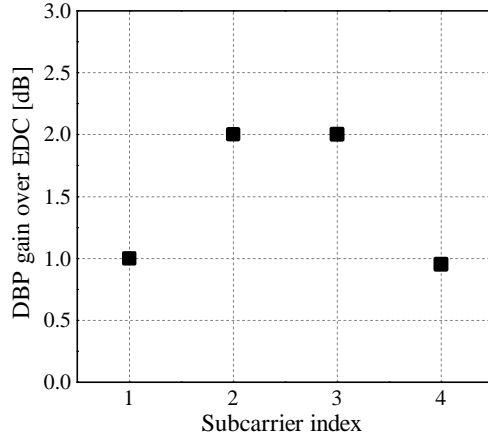


Fig. 5. DBP gain over EDC for each subcarrier of the superchannel after 5,000 km of optical fiber transmission.

as the 100 km span in our re-circulation loop comprises 6 different fiber spools with different dispersion parameters, equalization enhanced phase noise (EEPN) [25], which arises from the interaction between laser phase noise and dispersion (not considered in this work), and the frequency-dependent ENOB of the receiver. Furthermore, different transmission distances were also experimentally investigated (see Fig. 6(b)). For shorter distances at higher signal launch powers, the inaccuracy between the model and the simulations with the experimental results was much smaller than the one presented in Fig. 4(b). This is expected from theory; the relative impacts of EEPN, or indeed variations in fiber chromatic dispersion, are negligible.

The experimentally measured SNR after 5,000 km for each subcarrier is shown in Fig. 5. A DBP gain of 2 dB was measured for subcarrier 2 and 3, while the DBP gain for the outer subcarriers 1 and 4 was only 1 dB as the transceiver noise is higher for those channels.

To further support the theoretical considerations and to investigate the impact of transceiver noise on DBP gain, the maximum SNR as a function of distance (100 km to 5,000 km) is shown in Fig. 6. First an ideal scenario, without transceiver noise, was considered as shown in Fig. 6(a). As expected and as is well-known from previous reports [6, 12, 19] of studies on ideal systems, DBP yields impressive gains in SNR, particularly for shorter distances. However, as shown in Fig. 6(b), systems with limited transceiver SNR, the DBP gain for short distances is smaller, as the transceiver noise is the predominant noise.

The observation is supported by experimental data (markers), with an excellent agreement. For this particular system a 150% increase in reach (from 1,000 km to 2,500 km) was measured experimentally; the same gain was observed in simulations including PMD. The results also suggest that DBP performance is, in fact, more limited by the noise imposed by the coherent optical transceivers than by stochastic effects like PMD, where the penalty is almost negligible (<0.2 dB) for transmission over 2,500 km.

The analytical model, simulations and experiments are all in excellent agreement. This stresses the significant impact of the transceiver noise on the gains achievable by DBP.

5. Analytical case study: C-band transmission

This section is dedicated to investigating the implications of transceiver noise on the performance of DBP on a fully-loaded C-band system using the analytical model described in Section 2. Firstly, the DBP gain as a function of number of backpropagated channels is analysed. Secondly, the impact of the transceiver noise ratio between transmitter and receiver on DBP performance is

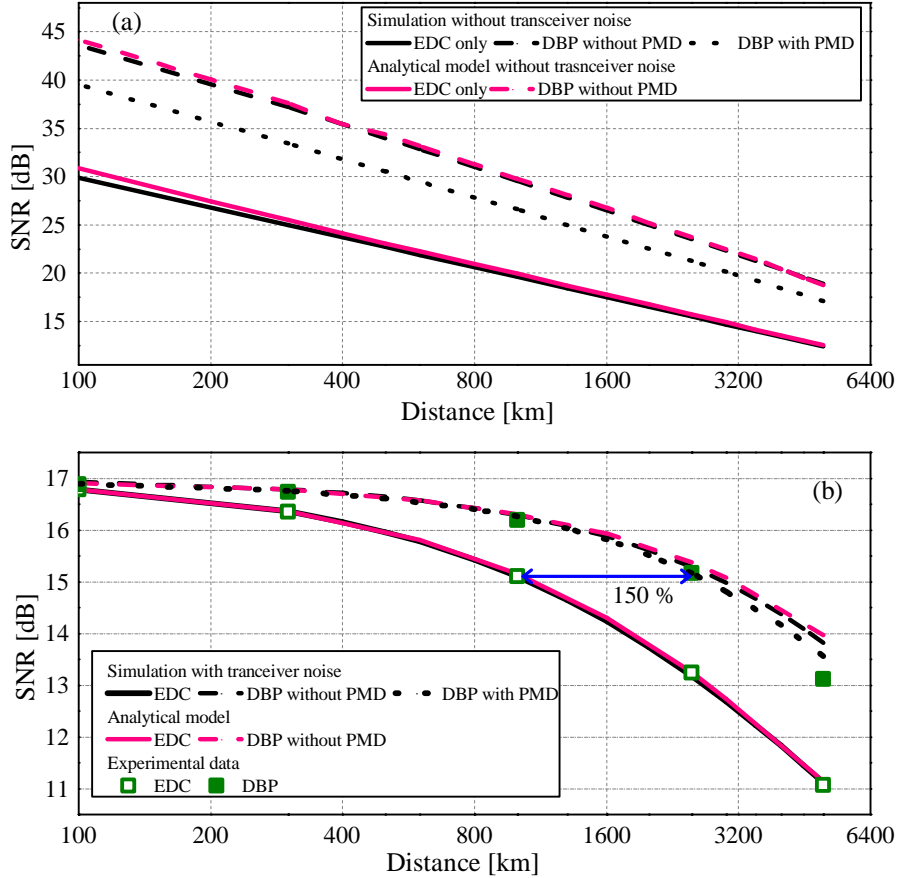


Fig. 6. SNR vs. distance at optimum subcarrier launch power(a) without transceiver noise and (b) with transceiver noise.

demonstrated. Finally, the contributions of transceiver noise-signal beating and ASE noise-signal beating is investigated. The system under consideration contains 155 Nyquist spaced 32 GBd channels with DP-64QAM modulation occupying an optical bandwidth of approximately 5 THz. The optical fiber link considered has the same specification as described in Section 3. This investigation was carried out for two different distances: 1,000 km and 10,000 km, which are representative of metropolitan area and ultra-long-haul/submarine links, respectively.

The SNR gain for receiver-side DBP with respect to EDC as a function of the number of backpropagated channels is shown in Fig. 7, for an ideal system, without transceiver SNR limit (black line) and for a transceiver limited SNR of 24 dB with transceiver noise located only at the transmitter (no transceiver noise-signal beating - blue line) and with the noise located only at the receiver (with transceiver noise-signal beating - red line). A higher transceiver SNR of 24 dB was chosen because it has been recently reported in [1, 27]. Fig. 7(a) shows the SNR gain over EDC after a 1,000 km transmission distance; a drastic decrease of 5.0 dB in SNR gain for FF-DBP is observed when all the transceiver noise is located at the transmitter (resulting in no transceiver noise-signal beating). This penalty is due to linear impairments only. This linear impairment is given by the transceiver limited SNR, which in this case is 24 dB; it sets the highest achievable SNR in the system and could already be estimated from the previous model as described in Section 2. A further decrease in SNR gain of 1.2 dB is observed for the case

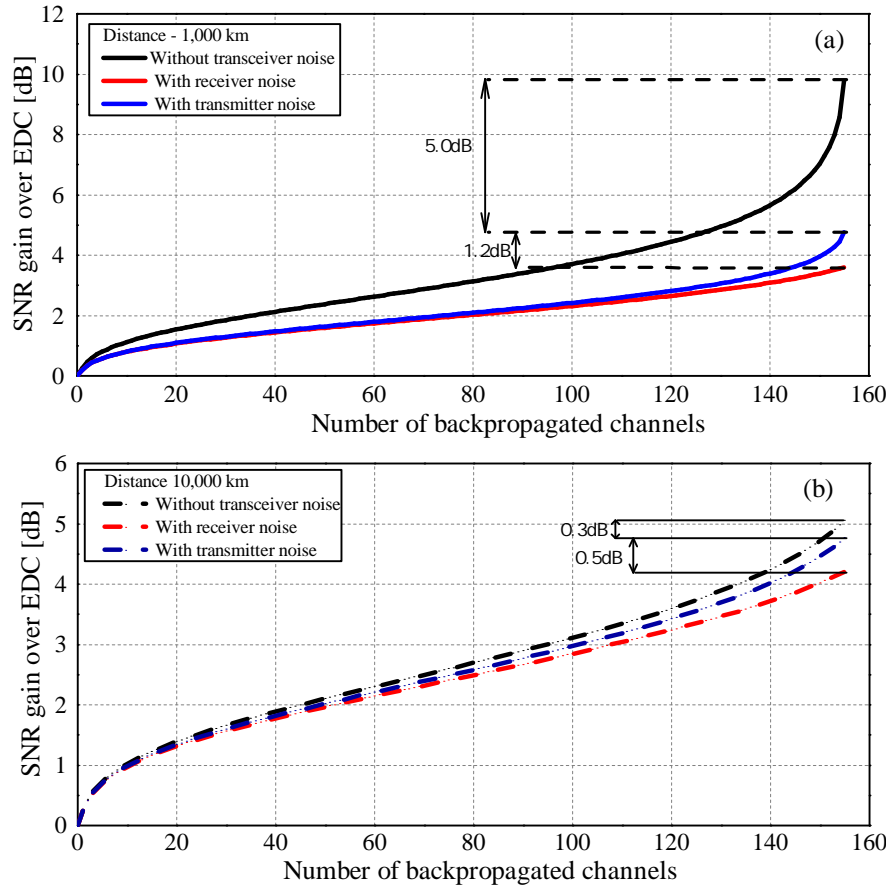


Fig. 7. SNR gais over EDC vs. number of backpropagated channels for transceiver SNR of 24 dB and transmission distance over (a) 1,000 km (b) 10,000 km.

when the transceiver noise is located only at the receiver. This decrease in SNR gain compared with transmitter noise only is due to the nonlinear beating between the receiver noise-signal. It is concluded that transceiver noise puts severe limitations on the gains that can be achieved by DBP. However, when a transpacific link with 10,000 km is considered, as shown in Fig. 7(b), the transceiver SNR has a minimal effect on DBP performance; for FF-DBP, we observed 0.3 dB and 0.8 dB decrease in SNR gain for transmitter noise and receiver noise, respectively compared to the idealized system. This is because the SNRs after the transmission are well below the transceiver SNR limitation.

5.1. Impact of the transceiver noise ratio between transmitter and receiver

In the previous Section the impact of the proposed nonlinear beating between transceiver noise-signal was demonstrated for the extreme case, with all the noise located at the receiver. To investigate the implications of the proposed nonlinear beating as a function of the ratio of the transceiver noise between the transmitter and the receiver, Fig. 8 illustrates the SNR gain for receiver-side FF-DBP (red line) and transmitter-side DBP (blue line) with respect to EDC as a function of the transceiver noise ratio between the transmitter and receiver. It considered a transceiver SNR of 24 dB. At '0', all the noise is located at the transmitter, '0.5' the noise is equally between the transmitter and receiver and '1' the transceiver-noise is located only

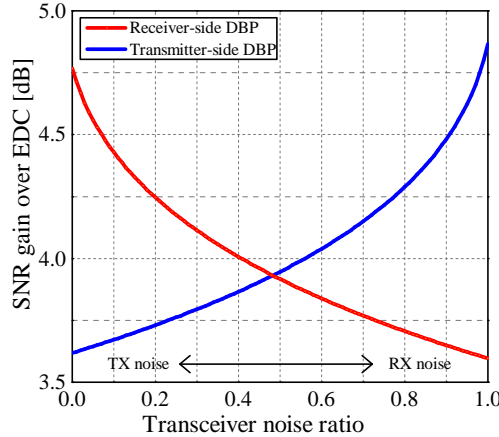


Fig. 8. The SNR gain for receiver-side FF-DBP (red line) and transmitter-side DBP (blue line) with respect to EDC as a function of the transceiver noise ratio between the transmitter and receiver.

at the receiver. A transmission distance of 1,000 km was considered. When the transceiver noise is located only at the transmitter, the receiver-side DBP can fully compensate for the arising transmitter noise-signal interactions and the gain is highest. The noise introduced by the transmitter beats with the signal along the entire physical (forward) link but this beating process is reversed in the backward (virtual) link that is introduced by DBP. In this case the SNR gain over EDC can be predicted by models already available in the literature as described in Section 2. However, when a part of the transceiver noise contribution comes from the receiver, the receiver-side DBP introduces (virtual) receiver noise-signal beating in the backward transmission link of DBP. Therefore, the gain is minimal as there is uncompensated transceiver noise beating. A gradual increase in the distribution of the noise towards the receiver decreases the DBP gain over EDC. For instance, receiver-side DBP gives a gain of 4.8 dB when all the transceiver noise is located at the transmitter; this gain decreases to 3.9 dB when the ratio of the transceiver noise is equally distributed between transmitter and receiver. A further reduction in the gain, to only 3.6 dB is achieved if the transceiver noise is located only at the receiver. The same analysis and opposite conclusion can be made for transmitter-side DBP (blue line).

5.2. Transceiver noise-signal beating in a C-band transmission system

In this subsection the contributions of transceiver noise-signal beating and the ASE noise-signal beating are investigated in more detail for the C-band system described above. The transceiver noise was considered equally split between transmitter and receiver. SNR gains for receiver-side DBP with respect to EDC as a function of transceiver SNR are shown in Fig. 9(a) and (b) for transmission over 1,000 km and 10,000 km, respectively. The green line shows the SNR predicted by the model according to (8) and the orange line shows the resulting SNR when ASE noise-signal interactions are set to zero. Moreover, the vertical lines show the transceiver SNR value where the amount of ASE noise-signal beating equals the amount of transceiver noise-signal beating as an exact solution (dotted line) and as an approximation (dashed line) taken from inequality (11).

It can be observed that the ASE noise-signal interactions are negligible when the transceiver SNR limit is around 26 dB for transmission over 1,000 km (Fig. 9(a)). For a transmission distance of 10,000 km as illustrated in Fig. 9(b), the ASE noise-signal interactions are negligible for a transceiver SNR of 10 dB (one order of magnitude) lower than the transceiver SNR that would

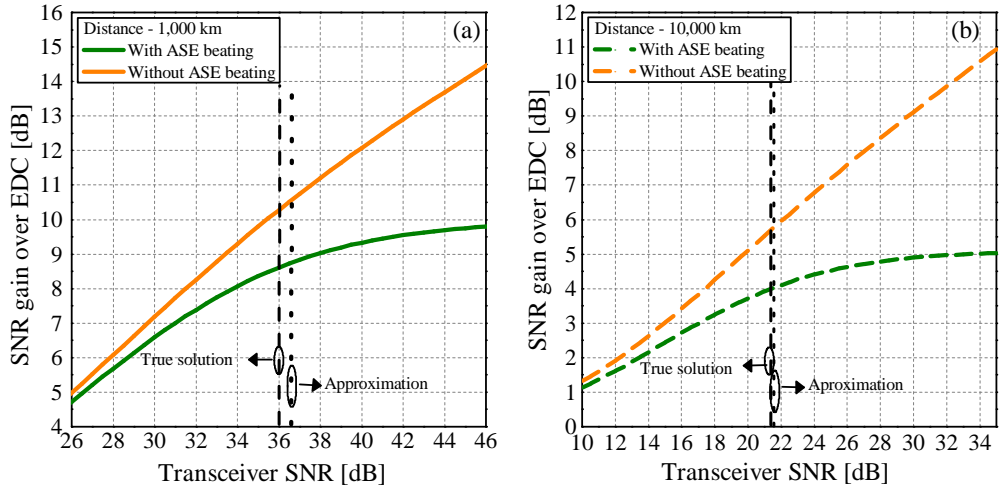


Fig. 9. SNR gains over EDC for different transceiver SNR's for transmission distance over (a) 1,000 km and (b) 10,000 km. The vertical lines show the true solution (dashed line) together with its approximation (dotted line) from Inequality (11) for the transceiver SNR where the ASE signal beating is equals the receiver noise-signal beating is shown by the vertical lines.

yield equal ASE noise signal-beating and transceiver noise-signal beating contributions. This is in good agreement with inequality (11) as the small mismatch of 0.5 dB is minor as compared to 10 dB. Therefore, the inequalities (11) and (12) in Section 2 serve as a simple but sufficient indicator about the negligible beating contributions. As argued previously, the technique of split DBP relies on sufficient ASE-signal actions and as shown in Fig. 9(a), for transmission over 1,000 km, a transceiver SNR of at least 36 dB is required to make split DBP beneficial over pure transmitter or receiver-side DBP. However, for transmission over 10,000 km (Fig. 9(b)), the required transceiver SNR must be at least 22 dB. Therefore, in realistic systems the technique of split DBP is expected to give more gains than transmitter-side DBP or receiver-side DBP when the inequality (11) is satisfied.

6. Conclusions

In this work, we presented a generalized expression to estimate the SNR for DBP in the presence of transceiver noise. This expression correctly accounts for nonlinear transceiver noise-signal beating in an optical fiber transmission link. The proposed model was compared with split-step simulation and experimental data and an excellent agreement was found. The results also suggest that, for a typical transmission system, DBP performance for distances smaller than approximately 5,000 km is more fundamentally limited by the noise imposed by the coherent optical transceivers than by the stochastic fiber channel impairment, PMD.

This simple expression enables, for the first time, the prediction of the DBP performance for any practical system, which is not dominated by PMD. It requires only the measured back-to-back SNR without any extrinsic noise sources, the fiber parameters and P_{ASE} estimation from the experimental configuration under test. Crucially, this model shows that the SNR gains from digital nonlinearity compensation can be significantly increased, provided the transceiver noise can be reduced.

Funding

This work was supported by the U.K. Engineering and Physical Sciences Research Council (EPSRC) under Grant EP/J017582/1 (UNLOC).

Acknowledgement

The authors wish to thank Dr Sergejs Makovejs and Corning Inc. for supplying the Corning® Vascade® EX2000 fiber span used in this work. An Engineering and Physical Sciences Research Council (EPSRC) Doctoral Training Partnership (DTP) studentship to Daniel Semrau is gratefully acknowledged. Note, the the authors marked † contributed equally to this paper.

Appendix

In this section the inequalities (11) and (12) are derived. For typical parameter values in optical communication, $\Gamma \gg 1$ (cf. (6)). Furthermore, the relations $\cosh(x) \approx \exp(x)/2$ for $x \gg 0$ and $\text{acosh}(\Gamma) \approx \ln(2\Gamma)$ for $\Gamma \gg 1$ are used to obtain an approximation of (9), which yields $\phi \approx (2\Gamma)^{\frac{1}{3}} - 1$. Substituting in the exact expression for the optimum launch power (7) and applying (10) yields

$$P_{\text{opt}} \approx \left(\frac{P_{\text{ASE}}}{6N^\epsilon \kappa_R \eta} \right)^{\frac{1}{3}} - \frac{\xi_1 P_{\text{ASE}}}{6N^{1+\epsilon} \kappa_R}. \quad (13)$$

To show (11), we first conclude from the last term in the denominator of (5) that receiver noise-signal interactions can be neglected if

$$\xi_1 P_{\text{ASE}} \gg N^{1+\epsilon} \kappa_R P_{\text{opt}}. \quad (14)$$

Inserting (13) in (14) and rearranging yields

$$(7\xi_1)^3 P_{\text{ASE}}^2 \eta \gg 36N^{3+2\epsilon} \kappa_R^2. \quad (15)$$

For typical signals in optical fiber communications, the coherence factor ϵ is very small [16]. When $\epsilon \approx 0$, ξ_1 can be approximated as $\xi_1 \approx N(N+1)/2$, or, assuming that $N \gg 1$, $\xi_1 \approx N^2/2$. Under these conditions, (15) can be expressed as

$$\left(\frac{4}{27P_{\text{ASE}}^2 \eta N^3} \right)^{\frac{1}{3}} \ll \frac{7}{6(3\kappa_R)^{\frac{2}{3}}}, \quad (16)$$

where we recognize the left-hand side of (14) as (4) with $\kappa = 0$, i.e., the SNR when EDC only is applied in the absence of any transceiver limitation, which we denote by $\text{SNR}_{\text{EDC,ideal}}$. Furthermore, assuming that the transceiver noise is equally split between transmitter and receiver, $\text{SNR}_{\text{TR}} = 2/\kappa_R$, and (16) becomes

$$\text{SNR}_{\text{EDC,ideal}} \ll \frac{7}{6^{\frac{5}{3}}} \text{SNR}_{\text{TR}}^{\frac{2}{3}}. \quad (17)$$

Converting (17) to a decibel scale yields (11).